Research Article

Journal of PeptideScience

Received: 29 July 2009 Revised: 11 April 2010 Accepted: 17 April 2010 Published online in Wiley Interscience: 27 May 2010

(www.interscience.com) DOI 10.1002/psc.1251

Effects on *in vitro* and *in vivo* angiogenesis induced by small peptides carrying adhesion sequences

Maria Teresa Conconi,[a]* ‡ Francesca Ghezzo,[b]‡ Monica Dettin,[b] Luca Urbani,[a] Claudio Grandi,[a] Diego Guidolin,[c] Beatrice Nico,[d] Carlo Di Bello,[b] Domenico Ribatti[d] and Pier Paolo Parnigotto[a]

It is well known that tumor growth is strictly dependent on neo-vessel formation inside the tumor mass and that cell adhesion is required to allow EC proliferation and migration inside the tumor. In this work, we have evaluated the *in vitro* and *in vivo* effects on angiogenesis of some peptides, originally designed to promote cell adhesion on biomaterials, containing RGD motif mediating cell adhesion via integrin receptors [RGD, GRGDSPK, and $(GRGDSP)_4K$] or the heparin-binding sequence of human vitronectin that interacts with HSPGs [HVP(351–359)]. Cell adhesion, proliferation, migration, and capillary-like tube formation in Matrigel were determined on HUVECs, whereas the effects on *in vivo* angiogenesis were evaluated using the CAM assay. $(GRGDSP)_4K$ linear sequence inhibited cell adhesion, decreased cell proliferation, migration and morphogenesis in Matrigel, and induced anti-angiogenic responses on CAM at higher degree than that determined after incubation with RGD or GRGDSPK. Moreover, it counteracted both *in vitro* and *in vivo* the pro-angiogenic effects induced by the Fibroblast growth factor (FGF-2). On the other hand, HVP was not able to affect cell adhesion and appeared less effective than $(GRGDSP)_4K$. Our data indicate that the activity of RGD-containing peptides is related to their adhesive properties, and their effects are modulated by the number of cell adhesion motifs and the aminoacidic residues next to these sequences. The anti-angiogenic properties of $(GRGDSP)_4K$ seem to depend on its interaction with integrins, whereas the effects of HVP may be partially due to an impairment of HSPGs/FGF-2.

Keywords: angiogenesis; cell adhesion; RGD; heparin-binding motif; FGF-2

Introduction

Angiogenesis is a process that leads to the formation of new vessels from pre-existing ones, such as capillary and post-capillary venules [1]. It can occur through endothelial sprouting or intussusceptive (non-sprouting) microvascular growth [2]. The latter mechanism is not dependent on local EC proliferation and involves the division of large sinusoidal capillary into smaller capillaries. On the contrary, sprouting angiogenesis is a multi-step process, where EC migration and proliferation are tightly controlled by a balance of pro- and anti-angiogenic factors. The basement membrane is degraded by proteolytic enzymes, such as matrix metalloproteinases and plasminogen activators, to allow the migration of ECs into the perivascular stroma. The angiogenic stimuli activate ECs that proliferate and then organize into tubular structures leading to the development of a circulatory network. Finally, neo-vessels are stabilized by the perivascular apposition of smooth muscle cells and pericytes that together with ECs synthesize the basement membrane constituents [3].

Angiogenesis is involved in numerous biological processes, such as embryogenesis, tissue remodeling, the female reproductive cycle, and wound healing [4]. However, several diseases arise from an impairment of the angiogenic process: a down-regulation leads to disorders characterized by ischemia, such as chronic wounds and obstructive cardiovascular diseases [4,5], whereas an excessive neo-vessel formation is involved in the pathogenesis of a variety of diseases, such as rheumatoid arthritis, psoriasis, diabetic retinopathy, and tumor growth [4,6]. Fibroblast growth factor (FGF)-2, a pro-angiogenic factor, is highly expressed in patients with highly vascularized and advanced cancers, and its expression level has been correlated with cancer progression and metastasis [7].

* *Correspondence to: Maria Teresa Conconi, Department of Pharmaceutical Sciences, School of Pharmacy, University of Padua, via Marzolo 5, 35131 Padua, Italy. E-mail: mariateresa.conconi@unipd.it*

a *Department of Pharmaceutical Sciences, School of Pharmacy, University of Padua, via Marzolo 5, 35131 Padua, Italy*

b *Department of Chemical Process Engineering, School of Engineering, University of Padua, via Marzolo 9, 35131 Padua, Italy*

c *Department of Human Anatomy and Physiology, School of Medicine, University of Padua, via Gabelli 65, 35121 Padua, Italy*

d *Department of Human Anatomy and Histology, School of Medicine, University of Bari, Piazza G. Cesare 11, Bari, Italy*

‡ *These authors contributed equally to this work.*

Abbreviations used: *ECs, endothelial cells; ECM, extracellular matrix; HSPGs, heparin sulfate proteoglycans; HUVECs, human umbilical vein endothelial cells; CAM, chorioallantoic membrane.*

Since when Folkamn [8] demonstrated that the tumor growth depends on vascularization, and subsequently, it can be inhibited by a strict control of neo-vessel formation inside the tumor mass, several strategies aimed to counteract each step of the angiogenic process have been designed, developed, and evaluated both *in vitro* and *in vivo* [9]. Unsatisfactory results have been obtained using antagonists of angiogenic factors [10]. As tumor contains a heterogeneous population of cells whose genome is unstable, the expression pattern of pro-angiogenic factors can be altered during tumor progression leading to resistance. On the contrary, the inhibitors of angiogenesis affecting EC proliferation, migration, and differentiation would overcome such problem, because EC genome is stable. Among this group, several protein inhibitors and chemical compounds have shown to be effective in various animal tumor models [9].

Cell adhesion to macromolecules of the ECM is required to allow EC proliferation and migration inside the tumor. ECs can adhere by means of different mechanisms, such as (i) interaction with RGD (Arg-Gly-Asp) motif via cell membrane integrin receptors [11] and (ii) interaction between cell membrane HSPGs and heparin-binding sites on ECM proteins [12]. Thus, molecules containing these signal sequences can be used either in tissue engineering as adhesion factors, when absorbed or chemically bound to the surface of biomaterials [13], or as anti-angiogenic agents, when used as soluble factors, through a competition with ECM components for the binding to cell surface [14–16]. The loss of anchorage can induce pro-apoptotic signals inside ECs leading to an inhibition of angiogenic process [17].

Although both RGD and heparin-binding motifs are contained in several ECM macromolecules, the clinical use of large intact proteins is often strongly limited because they are often insoluble and unstable macromolecules. These problems can be overcome using small peptides containing only the sequence responsible for cell adhesion. Small peptides exhibit higher stability and are cheaper than proteins. Moreover, they can selectively target one particular type of cell adhesion receptors [18–21].

Starting from these considerations, we have evaluated the *in vitro* and *in vivo* effects on angiogenesis induced by four peptides (Table 1), originally designed to promote cell adhesion on biomaterials [22]. Three peptides contain the RGD motif, that mediates cell adhesion via cell membrane integrin receptors: (i) RGD as minimal active sequence, (ii) GRGDSPK reproducing the natural 6-mer sequence of the fibronectin added with a *C*-terminal Lys residue, and (iii) $(GRGDSP)_4K$ linear sequence carrying four GRGDSP sequences. The fourth peptide, HVP(351–359), presents the heparin-binding sequence of human vitronectin that interacts with cell membrane HSPGs. Among the tested peptides, $(GRGDSP)_4K$ appeared the most effective, because it exerted both *in vitro* and *in vivo* anti-angiogenic activity and was able to counteract the stimulatory effect induced by exogenous FGF-2.

Table 1. Sequences of synthetic peptides

Peptide	Sequence
RGD	RGD
GRGDSPK	GRGDSPK
$(GRGDSP)_4K$	GRGDSPGRGDSPGRGDSPGRGDSPK
HVP	FRHRNRKGY

Materials and Methods

Peptide Synthesis

All peptides were synthesized by solid-phase methods using a fully automated peptide synthesizer (Applied Biosystems, Model 431A) via Fmoc chemistry, as previously reported [22,23]. Crude products were purified using semi-preparative reversed-phase chromatography. Analytical RP-HPLC analysis, capillary electrophoresis (Applied Biosystems, Capillary electrophoresis system, model 430A), and mass spectrometry (Mariner Applied Biosystems, Foster City, USA) allowed to confirm the identity of synthetic products and their high homogeneity grade (over 98%).

Cell Culture

Umbilical cord was obtained, with the mother's consent, from Cittadella Hospital according to the guidelines established by the Italian Public Health Ministry. Primary cultures of HUVECs were obtained by the enzymatic digestion of umbilical vein endothelial layer with 0.1% collagenase IV solution (Sigma–Aldrich, Milan, Italy). The cells were seeded on Petri dishes (BD Biosciences, Franklin Lakes, NJ, USA) previously coated with fibronectin (1 μg/ml; Sigma) and grown with culture medium composed of endothelial cell growth medium MV_2 (Promocell, Heidelberg, Germany), 5% FCS, and endothelial MV_2 medium kit (Promocell) containing 1 μg/ml ascorbic acid, 10 ng/ml hFGF-2, 5 ng/ml hEGF, 0.2 μg/ml hydrocortisone, 20 ng/ml R^3-IGF-1, 0.5 ng/ml VEGF. Cultures were incubated at 37 °C in a humidified atmosphere. HUVECs were used up to the fifth passage and harvested at 80% confluence. Basal medium composed only of endothelial cell growth medium MV_2 without FCS and growth factors was mainly used for the experiments.

Cell Adhesion

Wells of a 48-well non-tissue culture treated plate (BD Biosciences) were previously conditioned with the peptides (2 nmol/cm^2) by incubation at 37 °C for 24 h. At the end of the incubation period, the peptide solutions were removed, the wells were washed with PBS, and aspecific sites were blocked with 1 mg/ml BSA solution for 2 h at 37 °C. HUVECs (3×10^4 cells/cm^2) were seeded using basal medium and then, the cells were allowed adhering for 3 h under standard tissue culture conditions. At the end of the incubation period, non-adherent cells were carefully removed by washing twice with phosphate buffer (PBS) and the adherent cells were fixed on 10% formaldehyde in phosphate buffer overnight. ECs adhesion was quantified by counting the number of cells in five random fields per well (100× magnification). The same assay was also performed seeding HUVECs (3×10^4 cell/cm^2) in culture medium, with or without RGD, GRGDSPK, $(GRGDSP)_4K$, and HVP (0.1 mM) onto 48-well non-tissue culture treated plates. The number of adherent cells was determined as described above. Results, means of three experiments, were expressed as number of cells.

Cell Proliferation

HUVECs (2×10^4 cell/cm^2) were seeded on a 96-well plate (BD Biosciences), and after a 24-h incubation period, cultures were washed with PBS and the culture medium was replaced with basal medium, with or without RGD (0.1 and 0.025 mM), GRGDSPK (0.1 and 0.025 mM), $(GRGDSP)_4K$ (0.1 and 0.025 mM), HVP (0.1 and

Journal of PeptideScience

0.025 mM), FGF-2 (50 ng/ml, R&D Systems, Abington, UK), and FGF-2 plus each peptide (0.1 mM). After 20-, 44-, and 68-h incubation periods, cells were treated with MTT (0.5 mg/ml, Sigma) for 4 h. Formazane precipitates were dissolved in 2-propanol acid (0.04 M HCl in 2-propanol; Sigma) and optical density was measured at 570 nm, using a Microplate autoreader EL 13 (BIO-TEK Instruments Inc., Winooski, Vermont USA). Results were expressed as cell number or percent change from control cultures grown with basal medium. The linearity of absorbance of formazan over a range of $5 \times 10^3 - 50 \times 10^4$ cells was established by determining the linear coefficient (0.9858).

Cell Apoptosis

HUVECs (2×10^4 cell/cm^2) were seeded on a 96-well plate and incubated overnight at 37 °C. Then, cells were washed and treated for 24 h with RGD, GRGDSPK, $(GRGDSP)_4K$, or HVP (0.1 mM) dissolved in basal medium. Apoptosis was detected by an enzyme-linked immunoassorbent assay (ELISA) using the Cell Death Detection ELISA^{PLUS} Kit (Roche Molecular Biochemicals, Mannheim, Germany). At the end of the incubation period, cells were lysated and then centrifuged. Aliquots of supernatant were transferred to a streptavidin-coated well of a microtiter plate. Apoptosis detection was based on a quantitative sandwich-enzyme immunoassay using peroxidase-labeled monoclonal antibodies directed against DNA and histones of mono- and oligo-nucleosomes in supernatants of cell lysates. Peroxidase retained in immunocomplexes was measured photometrically at 405 nm wavelength using 2,2′-azino-di-[3-ethylbenzthiazoline sulfonate(6)]diammonium salt as substrate. Results were expressed as percent change from control cultures grown with basal medium.

Cell Necrosis

As described above, HUVECs (2×10^4 cell/cm^2) were seeded on a 96-well plate and treated for 24 h with RGD, GRGDSPK, $(GRGDSP)_4K$, and HVP (0.1 mM) dissolved in basal medium. Cell death (necrosis) was determined by measuring the release of lactate dehydrogenase (LDH), using the Roche LDH-Cytotoxicity detection kit. Briefly, the activity of LDH was determined by measuring its ability to reduce tetrazolium salt to formazan, in the presence of NAD^+ and diaphorase. Formazan production was determined by measuring absorbance at 490 nm wavelength. Results were expressed as percent change from control cultures grown with basal medium.

Cell Migration

Cell migration was evaluated using a modified Boyden chamber. HUVECs (3×10^4 cell/cm^2) were seeded on the upper side of 5.0 μm pore Transwell insert (Corning Inc.) in basal medium supplemented with 1% FCS with or without the tested peptides (0.1 or 0.025 mM). Inserts were placed in a 24-well plate containing medium supplemented with growth factors (lower chamber). After 4 h, cultures were fixed on 10% formaldehyde (Sigma) and the upper membrane of the insert was swabbed to remove non-migrated cells. The membrane was cut from the insert and mounted with DAPI. HUVECs migration was quantified by counting the number of nuclei in the lower side of the membrane in five random fields per insert (magnification of 100×) by fluorescence microscopy. Experiments were repeated five times. Results were expressed as percent change from control cultures incubated with basal medium supplemented only with growth factors.

In vitro Morphogenesis

Matrigel (BD Biosciences) was thawed on ice overnight, spread evenly over each well (50 μl) of a 24-well plate, and allowed to polymerize for 30 min at 37 °C. HUVECs were seeded (4×10^4 cell/cm^2) in basal medium supplemented with 1% FCS and with or without RGD, GRGDSPK, $(GRGDSP)_4K$, and HVP (0.1 and 0.025 mM), FGF-2 (50 ng/ml), and FGF-2 plus peptides (0.1 and 0.025 mM).

After 18 h of incubation at 37 °C, cultures were fixed on 2% glutaraldehyde (Sigma) in cacodylate buffer, pH 7.2 and then photographed (5 fields for each well: the four quadrants and the center) at a ×50 magnification. Phase-contrast images were recorded using a digital camera (DS camera system; Nikon Instruments Inc., Firenze, Italy) connected to a Leica DMIR2 HC Fluo inverted microscope (Leica Microsystems, Milan, Italy) and saved as TIFF files. Image analysis was carried out using the Qwin image analysis software (Leica Imaging System), as previously detailed [24], and the following dimensional parameters (percent area covered by HUVECs and total length of HUVECs network per field), and topological parameters (number of meshes and branching points per fields) were estimated. Values were expressed as percent change from control cultures grown with basal medium supplemented with 1% FCS.

In vivo CAM Assay

Fertilized White Leghorn chicken eggs (20 for each experimental group) were incubated at 37 °C at constant humidity. On day 3 of incubation, a square window was opened in the egg shell and 2–3 ml of albumen was removed off so as to detach the developing CAM from the shell. The window was sealed with glass and the eggs were returned to the incubator. On day 8, sterilized gelatin sponges (1 mm^3) adsorbed with 0.1 mM RGD, $(GRGDSP)_4K$, HVP, alone/or with 200 ng/embryo of FGF-2 dissolved in 1 μl PBS were implanted on day 8 on the top of some CAM, as previously reported [25]. FGF-2 and PBS alone were used as positive and negative control, respectively. CAM were examined daily until day 12 and photographed *in ovo* with a stereomicroscope equipped with a Camera System MC 63 (Zeiss, Oberkochen, Germany). Blood vessels entering the implants or the sponges within the focal plane of the CAM were counted by two observers in a double-blind fashion at ×50 magnification.

Statistical Analysis

All results were expressed as mean ± SD of three separate experiments. Their statistical comparison was performed by analysis of variance, followed by Student's *t*-test.

Results and Discussion

Starting from the consideration that EC adhesion represents a starting point of angiogenic process and it is required to allow EC proliferation and migration inside the tumor, in this work, we have evaluated the effects on angiogenesis of four small peptides containing sequences responsible for cell adhesion via integrin or cell membrane HSPG interaction.

Our data indicate that the effects of RGD-containing peptides depends on (i) the number of cell adhesion motifs (GRGDSPK vs $(GRGDSP)_4K$) and (ii) the aminoacidic residues next to these sequences (RGD vs GRGDSPK).

Table 2. HUVEC adhesion on not tissue culture treated plates

Peptide	Cell number ± SD[a]	Cell number ± SD[b]
None	1.0 ± 0.3	361.0 ± 5.7
RGD	0	362.0 ± 15.1
GRGDSPK	0	315.0 ± 68.6
$(GRGDSP)_4K$	118.0 ± 22.6*[c]	10.0 ± 3.5*
HVP	1.0 ± 0.4[c]	333.0 ± 35.8

Results, means of three separate experiments, are expressed as cell number ± SD.
[a] Using basal medium, cells were seeded on plates previously coated with peptides (2 nmol/cm^2).
[b] Using culture medium containing 0.1 mM peptides, cells were seeded on non-coated plates.
[c] Data reported from Dettin *et al*. [26.]
* $p < 0.05$ versus control cultures, Student's *t*-test.

To evaluate whether the peptides adsorbed on the surface of the culture plates could enhance cell adhesion, cells were seeded on non-tissue culture plates using basal medium, thus avoiding FCS-induced cell adhesion. In this experimental conditions, neither RGD and GRGDSPK was able to increase EC adhesion (Table 2, column A). On the contrary, our previous data [26] have shown that $(GRGDSP)_4K$ enhances cell adhesion compared to that determined in control cultures, whereas HVP is ineffective. On the other hand, when peptides were added to the basal medium and not adsorbed on culture wells, no variations were detected in comparison with the control where adhesion rate was very low. So, we decided to carry out other experiments using culture medium containing FCS and growth factors. As shown in Table 2 (column B), only $(GRGDSP)_4K$ significantly prevented HUVEC adhesion. This finding agrees to our previous observation carried out on rat osteoblast-like and porcine aortic EC cultures [22,23]. Our results suggest that the effects of peptides in the angiogenic process could be related to their adhesive properties. Indeed, adhesion assay clearly showed that only $(GRGDSP)_4K$ was able to increase or inhibit EC adhesion on non-tissue culture plates when used as coating and soluble factor, respectively.

$(GRGDSP)_4K$ exerted *in vitro* a strong anti-angiogenic activity at higher degree than that determined after incubation with RGD, used as reference compound, and the other RGD-derived peptide. It decreased EC proliferation and migration, and capillary-like tube formation in Matrigel, whereas RGD did not affect cell proliferation and migration and showed only a mild inhibition of morphogenesis.

At all incubation times, cell proliferation was significantly ($p < 0.05$) decreased by both concentrations of GRGDSPK, $(GRGDSP)_4K$, and HVP in comparison with untreated cultures (Figure 1). Moreover, 0.1 mM HVP and the linear peptide containing four RGD motifs appeared more effective than GRGDSPK. On the contrary, no variation in cell growth was revealed after treatment with RGD.

These inhibitory effects were not connected to either apoptosis or necrosis induction, because GRGDSPK, $(GRGDSP)_4K$, and HVP (0.1 mM) decreased both the mono- and oligo-nucleosome formation (Figure 2A) and LDH release (Figure 2B) compared to that determined in non-treated cultures. These data suggest that other mechanisms, such as a slowing of cell cycle, could be involved.

HUVEC migration was inhibited only by 0.1 mM GRGDSPK and $(GRGDSP)_4K$, whereas lower concentrations were ineffective (Figure 3). No effect was visible after treatment with RGD and HVP.

After seeding on Matrigel, HUVECs spread and aligned with each other, giving rise within 18 h to tubule-like structures (Figure 4A). In the presence of GRGDSPK, cells were organized into a richer meshwork of capillary-like tubes than that observed in the control cultures (Figure 4B), whereas the incubation with $(GRGDSP)_4K$ (Figure 4C) and HVP (Figure 4D) produced meshwork disruption. Image analysis confirmed these observation, showing that 0.025 mM GRGDSPK significantly increased both dimensional (percent area covered by HUVECs and total length of the network per field) and topological parameters (number of meshes and branching points per field) of the capillary-like network and 0.1 mM GRGDSPK affected only the topological parameters (Figure 5A). On the contrary, 0.025 mM HVP (Figure 5B) and both concentrations of $(GRGDSP)_4K$ (Figure 5C) significantly decreased all the parameters, whereas 0.025 mM RGD induced a decrease only in topological parameters (Figure5D).

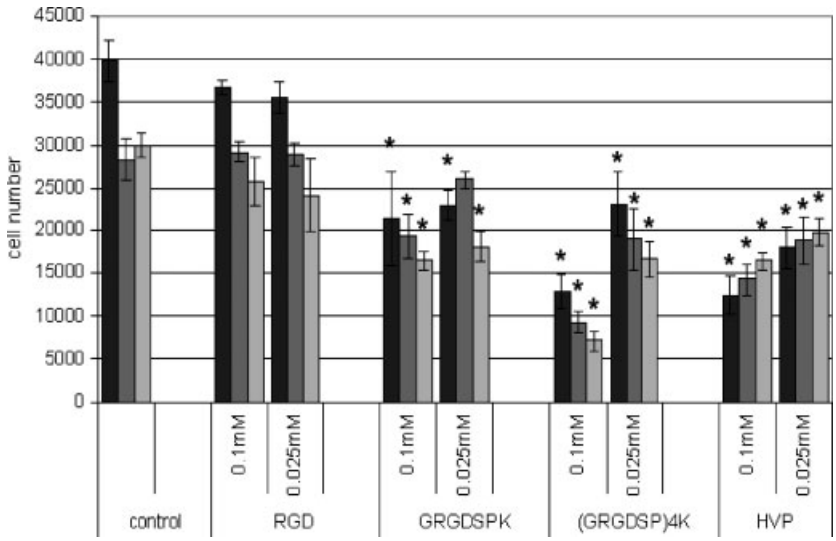

Figure 1. The cell proliferation in HUVECs was determined by the MTT assay after 24, 48 and 72 h of incubation with the peptides. Results were expressed as cell number. Bars (black = 24 h, dark gray = 48 h, light gray = 72 h) are means ± SD of three separate experiments. *$p < 0.05$ versus control cultures.

Journal of PeptideScience

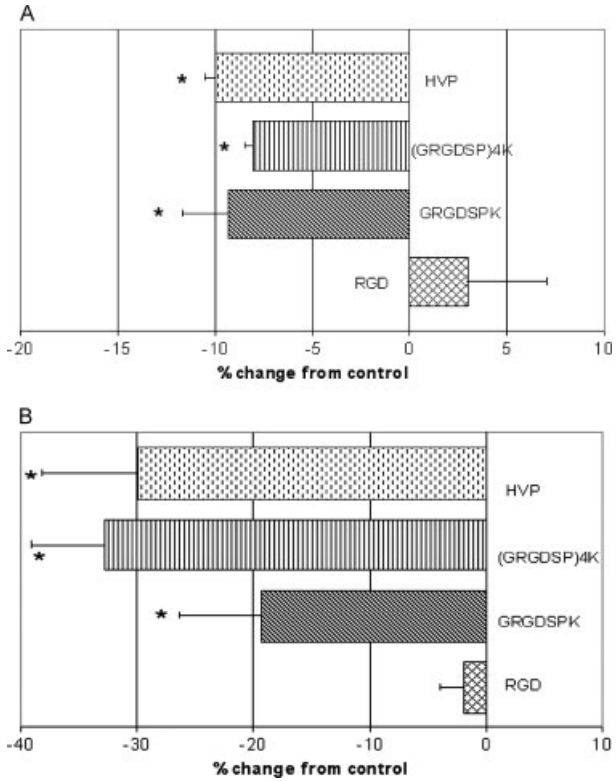

Figure 2. HUVECs were treated for 24 h with the peptides (0.1 mM). At the end of the incubation period, both apoptotic rate (A) and cell necrosis (B) were determined by the assessment of mono- and oligo-nucleosomes formation and LDH release, respectively. Results, expressed as percent change from control non-treated cultures (taken as 0), are the mean ± SD of three independent experiments. $^{*}p < 0.05$ versus control cultures, Student's *t*-test.

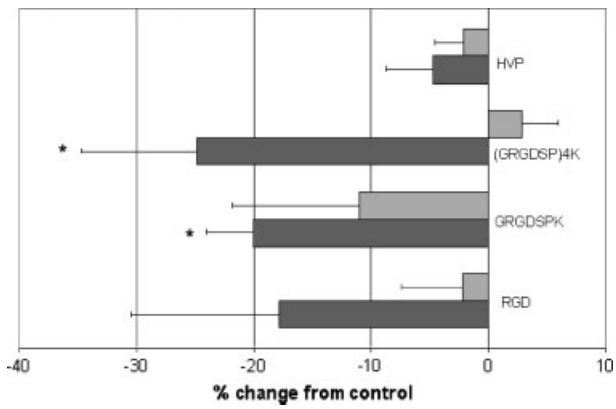

Figure 3. Cell migration of HUVECs through a 5.0 μm pore after 4 h from seeding with the tested peptides. Bars (dark gray = 0.1 mM, light gray = 0.025 mM) are means ± SD of three separate experiments. Results are expressed as percent change from control non-treated cultures (taken as 0). $^{*}p < 0.05$ versus control cultures.

Our data indicate that the repetition of signal sequences per chain enhances the *in vitro* anti-angiogenic activity. This result could be due to (i) the peptide structure that promotes a conformation more attractive to cells or (ii) the RGD clustering that allows integrin aggregation [27]. In fact, RGD functionalized biomaterials stimulate different cell responses not only by different average surface concentrations of ligands, but also by presenting the ligands in a way that allows integrin aggregation. Nanoscale RGD clustering seems to be a promising way to elicit cell responses mediated by integrin aggregation. As well-defined RGD arrangement on surfaces is hard to achieve, the use of multivalent RGD modified branched or repetitive linear molecule such as $(GRGDSP)_4K$ peptide could be a good alternative. The angiogenic effects can also be modulated by the aminoacidic residues next to the adhesion motif. Indeed, GRGDSPK reproducing the natural 6-mer sequence of the fibronectin added with a *C*-terminal Lys residue induced inhibition of EC proliferation, but unexpectedly enhanced morphogenesis on Matrigel. Now we cannot explain these contradictory results and further investigations will be needed.

Table 3. Effects of RGD, $(GRGDSP)_4K$, and HVP administered alone or in combination with FGF-2 on angiogenesis *in vivo* in the chick embryo CAM assay

Compound	Number of vessels
RGD	$4 \pm 2^{*}$
$(GRGDSP)_4K$	$3 \pm 1^{*}$
HVP	$4 \pm 2^{*}$
RGD + FGF-2	26 ± 3
$(GRGDSP)_4K$ + FGF-2	$15 \pm 4^{**}$
HVP + FGF-2	27 ± 4
FGF-2	28 ± 4
PBS	8 ± 2

$^{*}p < 0.001$ versus PBS, Student's *t*-test.
$^{**}p < 0.001$ versus FGF-2, Student's *t*-test.

In *in vivo* assays both RGD and $(GRGDSP)_4K$ elicited anti-angiogenic responses on CAM. Macroscopic observation of CAMs treated with 1 mM RGD, $(GRGDSP)_4K$, HVP alone showed that on day 12 of incubation, all peptides significantly inhibited physiological angiogenesis occurring in the sponges treated with vehicle alone (Table 3, Figure 6). This finding can be due to the longer incubation period used for *in vivo* assay compared to that used for *in vitro* morphogenesis assay.

$(GRGDSP)_4K$ effectively counteracted the increases in *in vivo* angiogenesis on CAM, cell proliferation, and capillary-like tube formation in Matrigel induced by FGF-2, that represents one the most important factors involved in the angiogenic process. On the contrary, other RGD-derived peptides were ineffective.

The increase in cell proliferation induced by FGF-2 was completely reversed by GRGDSPK, HVP, and $(GRGDSP)_4K$, that appeared particularly effective (Figure 7). In the same assay, RGD resulted ineffective.

As expected, 50 ng/ml FGF-2 increased the density of the meshwork of capillary-like structures (Figure 8). The stimulatory effect of FGF-2 was counteracted by 0.1 mM $(GRGDSP)_4K$, whereas the other peptides had no effects. Indeed, when FGF-2 was administered in the presence of $(GRGDSP)_4K$, both topological and dimensional parameters significantly decreased (Figure 8).

In CAM assay, when the peptides were added to a well-known angiogenic cytokine, namely FGF-2, only $(GRGDSP)_4K$ was able to significantly inhibit angiogenic response induced by FGF-2 (Table 3). Figure 6 shows numerous allantoic vessels developing radially toward the implants soaked with FGF-2, whereas $(GRGDSP)_4K$ partially inhibited the vascularization induced by the cytokine.

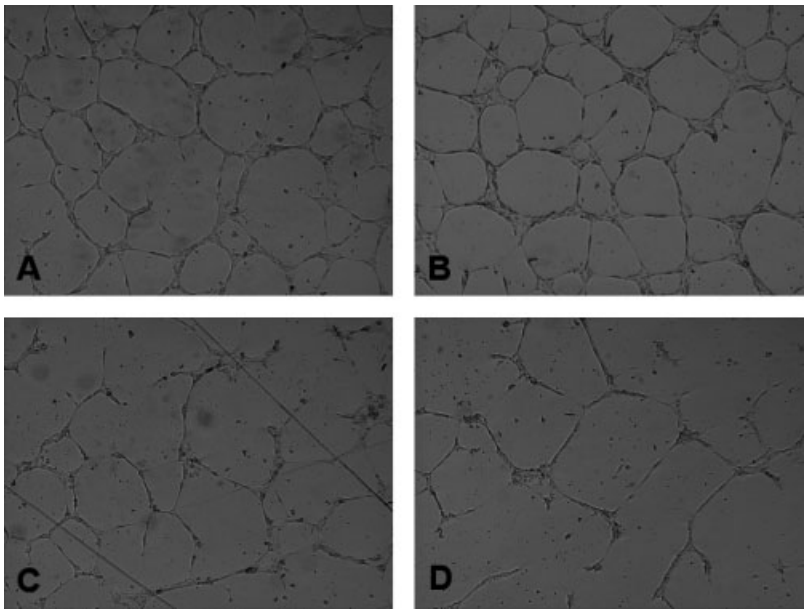

Figure 4. HUVECs were seeded on Matrigel and treated for 18 h with the peptides. Phase-contrast micrographs show the arrangement of HUVECs into a meshwork of capillary-like tubular structures when cultured on Matrigel for 18 h (A). GRGDSPK (0.025 mM) increased the density of the meshwork (B), whereas 0.025 mM $(GRGDSP)_4K$ (C) and 0.025 mM HVP (D) partially disrupted the meshwork. Magnification $\times 50$.

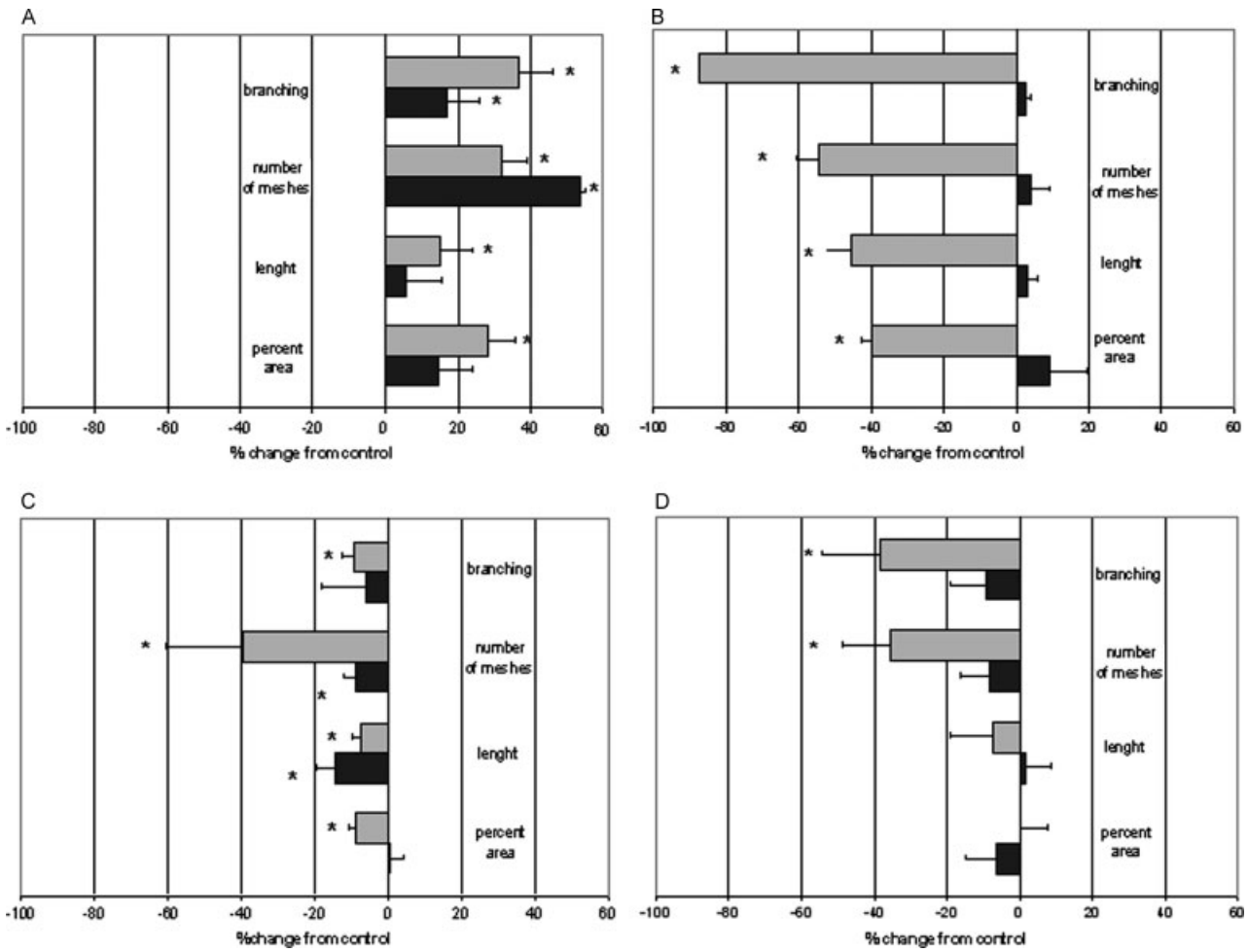

Figure 5. Quantitative analysis of the effects of GRGDSPK (A), HVP (B), $(GRGDSP)_4K$ (C), and RGD (D) on the dimensional (percent area covered by HUVECs and total length per field), and topological parameters (number of mesh per field and number of branching points per field) of the HUVEC meshwork. Results were expressed as percent change from control non-treated cultures (taken as 0). Bars (black = 0.1 mM, gray = 0.025 mM) are means ± SD of three separate experiments. $^*p < 0.05$ versus control cultures, Student's *t*-test.

Journal of PeptideScience

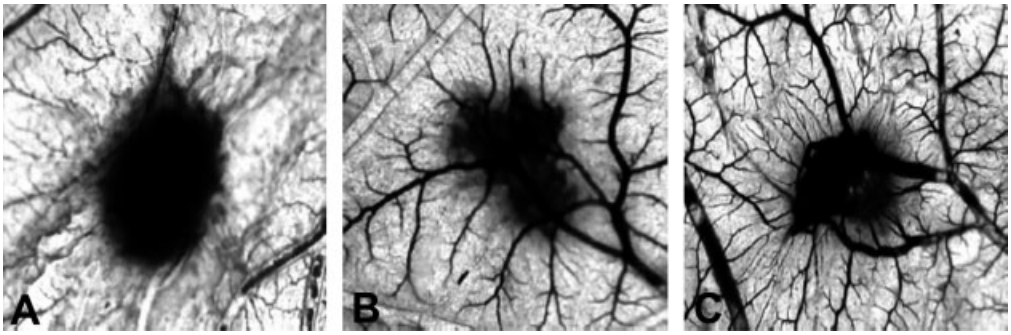

Figure 6. Macroscopic pictures of gelatin sponge soaked with $(GRGDSP)_4K$ (A), $(GRGDSP)_4K$ plus FGF-2 (B), and FGF-2 (C) implanted onto the chick embryo chorioallantoic membrane on day 12 of incubation. Magnification: ×50.

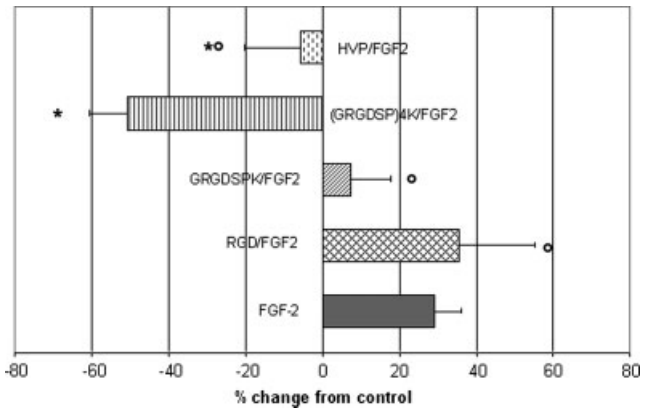

Figure 7. Cells were treated for 24 h with 50 ng/ml FGF-2 with or without 0.1 mM peptides. At the end of the incubation period, cell proliferation was determined by MTT assay. Results, expressed as percent change from control non-treated cultures (taken as 0), are the mean ± SD of three independent experiments. $^{*}p < 0.05$ versus FGF-2; $^{\circ}$ $p < 0.05$ versus $(GRGDSP)_4K$/FGF-2, Student's *t*-test.

Subsequently to its release from stromal and tumor cells, FGF-2 exerts its pro-angiogenic effects in an autocrine/paracrine manner, through interaction with tyrosin kinase receptors and activation of mitogen-activated protein kinase, protein kinase C, and various proteolytic systems [28]. FGF-2 exists mainly as immobilized molecule bound to the ECM and/or cell surface or as circulating complexes. Our data are consistent with the findings that the response of ECs to both free and immobilized FGF-2 can be also regulated by integrins [29]. Evidences suggest that the interaction between integrin $\alpha_v\beta_3$ and FGF-2 lead to the assembly of focal adhesion plaques containing $\alpha_v\beta_3$ and FGFR1, whose presence is required for the activation of ERK1/2 and cell proliferation [30]. In this context, several RGD-containing peptides able to inhibit FGF-2-dependent angiogenesis both *in vitro* and *in vivo* have been developed [31,32].

However, FGF-2 also interacts with the heparan sulfate glycosaminoglycan chains attached to HSPGs representing membrane-associated receptors or ECM components [33]. This interaction modulates FGF-2 biological activities both *in vitro* and *in vivo*, because it controls the bioavailability and EC interaction of the cytokine [34]. Moreover, HSPGs promote FGF-2 internalization

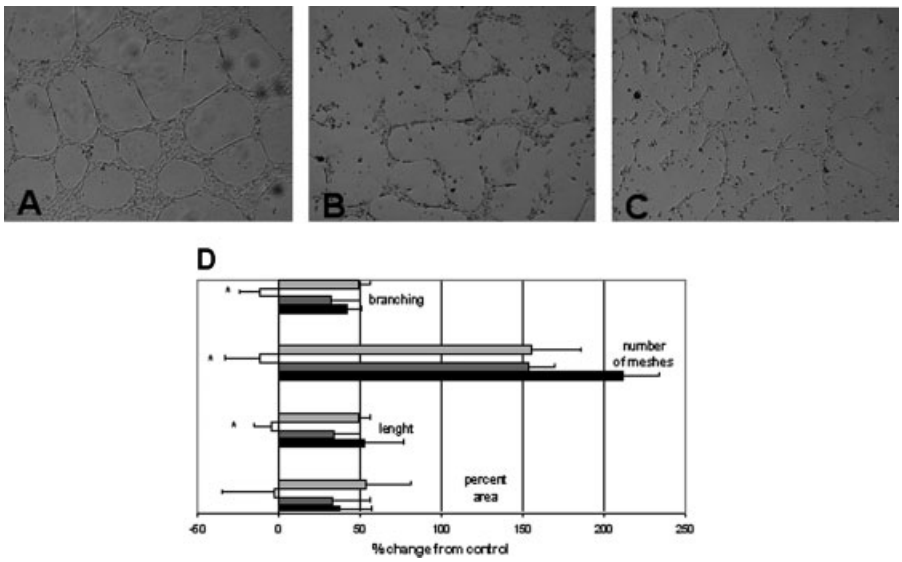

Figure 8. Effects of peptides on FGF-2-induced morphogenesis on Matrigel. Cells were treated for 18 h with 50 ng/ml FGF-2 with or without 0.1 mM peptides. Phase-contrast micrographs of HUVECs seeded on Matrigel and treated with 50 ng/ml FGF-2 (A), 0.1 mM $(GRGDSP)_4K$ (B), 50 ng/ml FGF-2 plus 0.1 mM $(GRGDSP)_4K$ (C). Magnification ×50. (D) Quantitative analysis of dimensional and topological parameters of the HUVEC meshwork. Results were expressed as percent change from control non-treated cultures (taken as 0). Bars (black, FGF-2; dark gray, RGD plus FGF-2; white, $(GRGDSP)_4K$ plus FGF-2; light gray, HVP plus FGF-2) are means ± SD of three separate experiments. $^{*}p < 0.05$ from FGF-2-treated cultures, Student's *t*-test.

and are required for a correct presentation of FGF-2 to its receptors [28]. Consequently, molecules, such as heparin-like anionic molecules [35,36], able to counteract the HSPGs/FGF-2 interaction may function as anti-angiogenic agents. In this context, HVP possesses the heparin-binding sequence present in human vitronectin and can interact with cell membrane HSPGs. HVP induced significant decreases in cell proliferation, inhibited morphogenesis on Matrigel and vessel formation on CAM when compared with that observed in non-treated control cultures. As it was not able to affect EC adhesion as previously reported [22] and here demonstrated, we can suppose that its anti-angiogenic properties may be due to an impairment of HSPGs/FGF-2 interaction inhibiting the autocrine–paracrine effects of the cytokine. Although, HVP completely reversed the increase in cell proliferation induced by FGF-2, it failed to counteract FGF-2-induced capillary-like tube formation in Matrigel and angiogenic response on CAM. To explain this result, it must be noted that molecules, such as HVP, containing heparin-binding sequences can modulate cell response to only immobilized FGF-2, whereas RGD-derived peptides can also act on free cytokine, as reported above. Moreover, the different manner by which FGF-2 was added in *in vitro* morphogenesis and cell proliferation assays may be, at least in part, responsible for these contradictory results: FGF-2 was added to cell suspension in the former assays and to adherent cultures 24 h after seeding in the latter ones.

The modulation of autocrine–paracrine effects of FGF-2 on ECs seems to be also involved in the decreases in cell proliferation revealed after treatment with HVP and $(GRGDSP)_4K$.

Collectively, our data indicate that the activity of RGD-containing peptides is related to their adhesive properties and their effects are modulated by the number of cell adhesion motifs. Indeed, $(GRGDSP)_4K$, carrying four GRGDSP sequences, exerts both *in vitro* and *in vivo* anti-angiogenic effects at higher degree than that determined after incubation with RGD or GRGDSPK. Its activity seems to be related to its interaction with cell membrane integrins resulting in an inhibition of both EC adhesion and FGF-2-induced angiogenic effects. On the other hand, HVP, carrying heparin-binding sequence, appeared less effective than $(GRGDSP)_4K$ and its effects could be probably mediated, at least in part, by an impairment of HSPGs/FGF-2 interaction. At present, we are planning further *in vivo* and *in vitro* experiments to evaluate whether $(GRGDSP)_4K$ could effectively inhibit tumor formation and deeply identify its molecular targets.

Acknowledgement

We would like to thank Lorenzo Tonin for his precious help and informatic support. This work was supported by MIUR Italy.

References

1 Risau W. Mechanisms of angiogenesis. *Nature* 1997; **386**: 671–674.
2 Burri PH, Hlushchuk R, Djonov V. Intussusceptive angiogenesis: its emergence, its characteristics, and its significance. *Dev. Dyn.* 2004; **231**(3): 474–488.
3 Ribatti D, Conconi MT, Nussdorfer GG. Nonclassic endogenous novel regulators of angiogenesis. *Pharmacol. Rev.* 2007; **59**: 185–205.
4 Liekens S, De Clercq E, Neyts J. Angiogenesis: regulators and clinical applications. *Biochem. Pharmacol.* 2001; **61**: 253–270.
5 Phelps EA, Garcia AJ. Update on therapeutic vascularization strategies. *Regen. Med.* 2009; **4**(1): 65–80.
6 Cao Y. Tumor angiogenesis and molecular targets for therapy. *Front. Biosci.* 2009; **14**: 3962–3973.
7 Cao Y, Cao R, Hedlund EM. R regulation of tumor angiogenesis and metastasis by FGF and PDGF signaling pathways. *J. Mol. Med.* 2008; **86**(7): 785–789.
8 Folkman J. Tumor angiogenesis: therapeutic implications. *N. Engl. J. Med.* 1971; **285**: 1182–1186.
9 Cao Y. Antiangiogenic cancer therapy. *Semin. Cancer Biol.* 2004; **14**: 139–145.
10 Garber K. Angiogenesis inhibitors suffer new setback. *Nat. Biotechnol.* 2002; **20**: 1067–1068.
11 Albelda SM, Buck CA. Integrins and other cell adhesion molecules. *FASEB J.* 1990; **4**: 2868–2880.
12 Mostafavi-Pour Z, Askari JA, Whittard JD, Humphries MJ. Identification of a novel heparin-binding site in the alternatively spliced IIICS region of fibronectin: roles of integrins and proteoglycans in cell adhesion to fibronectin splice variants. *Matrix Biol.* 2001; **20**(1): 63–73.
13 Huebsch JB, Fields GB, Triebes TG, Mooradian DL. Photoreactive analog of peptide FN-C/H-V from the carboxy-terminal heparin-binding domains of fibronectin supports endothelial cell adhesion and spreading on biomaterial surfaces. *J. Biomed. Mater. Res.* 1996; **31**: 555–567.
14 Swenson S, Ramu S, Markland FS. Anti-angiogenesis and RGD-containing snake venom disintegrins. *Curr. Pharm. Des.* 2007; **13**(28): 2860–2871.
15 Romanov VI, Goligorsky MS. RGD-recognizing integrins mediate interactions of human prostate carcinoma cells with endothelial cells in vitro. *Prostate* 1999; **39**: 108–118.
16 Vassilev TL, Kazatchkine MD, Van Huyen JD. Inhibition of cell adhesion by antibodies to Arg-Gly-Asp (RGD) in normal immunoglobulin for therapeutic use (intravenous imunoglobulin, IVIg. *Blood* 1999; **93**: 3624–3631.
17 Frisch SM, Screaton RA. Anoikis mechanisms. *Curr. Opin. Cell Biol.* 2001; **13**: 555–562.
18 Eichler J. Peptides as protein binding site mimetics. *Curr. Opin. Chem. Biol.* 2008; **12**(6): 707–713.
19 Rajesh BM, Iqbal J. Recent advances in the synthesis of some bioactive peptides and peptidomimetics. *Curr. Pharm. Biotechnol.* 2006; **7**(4): 247–259.
20 Gentilucci L, Tolomelli A, Squassabia F. Peptides and peptidomimetics in medicine, surgery and biotechnology. *Curr. Med. Chem.* 2006; **13**(20): 2449–2466.
21 Ruoslahti E. RGD and other recognition sequences for integrins. *Annu. Rev. Cell. Dev. Biol.* 1996; **12**: 697–715.
22 Dettin M, Conconi MT, Gambaretto R, Bagno A, Di Bello C, Menti AM, Grandi C, Parnigotto PP. Effect of synthetic peptides on osteoblast adhesion. *Biomaterials* 2005; **26**: 4507–4515.
23 Dettin M, Conconi MT, Gambaretto R, Pasquato A, Folin M, Di Bello C, Parnigotto PP. Novel osteoblast-adhesive peptides for dental/orthopedic biomaterials. *J. Biomed. Mater. Res.* 2002; **60**: 466–471.
24 Ribatti D, Guidolin D, Conconi MT, Nico B, Baiguera S, Parnigotto PP, Vacca A, Nussdorfer GG. Vinblastine inhibits the angiogenic response induced by adrenomedullin in vitro and in vivo. *Oncogene* 2003; **22**: 6458–6461.
25 Ribatti D, Nico B, Vacca A, Presta M. The gelatin sponge-chorioallantoic membrane assay. *Nat. Protoc.* 2006; **1**: 85–91.
26 Dettin M, Bagno A, Gambaretto R, Iucci G, Conconi MT, Tuccitto N, Menti AM, Grandi C, Di Bello C, Licciardello A, Polzonetti G. Covalent surface modification of titanum oxide with different adhesive peptides: surface characterization and osteoblast-like cell adhesion. *J. Biomed. Mater. Res. A* 2009; **90**(1): 35–44.
27 Hersel U, Dahmen C, Kessler H. RGD modified polymers: biomaterials for stimulated cell adhesion and beyond. *Biomaterials* 2003; **24**: 4385–4415.
28 Presta M, Dell'Era P, Mitola F, Moroni E, Ronca R, Rusnati M. Fibroblast growth factor/fibroblast growth factor receptor system in angiogenesis. *Cytokine Growth Factor Rev.* 2005; **16**: 159–178.
29 Sahni A, Francis CW. Stimulation of endothelial cell proliferation by FGF-2 in the presence of fibrinogen requires alpha(v)beta(3). *Blood* 2004; **104**: 3635–3641.
30 Tanghetti E, Ria R, Dell'Era P, Urbinati C, Rusnati M, Ennas MG. Biological activity of substrate-bound basic fibroblast growth factor (FGF-2): recruitment of FGF receptor-1 in endothelial cell adhesion contacts. *Oncogene* 2002; **21**: 3889–3897.

31 Presta M, Rusnati M, Urbinati C, Sommer A, Ragnotti G. Biologically active synthetic fragments of human basic fibroblast growth factor (bFGF): identification of two Asp-Gly-Arg-containing domains involved in the mitogenic activity of bFGF in endothelial cells. *J. Cell. Physiol.* 1991; **149**: 512–524.
32 Kumar CC, Malkowski M, Yin Z, Tanghetti E, Yaremko B, Nechuta T. Inhibition of angiogenesis and tumor growth by SCH221153, a dual alpha(v)beta3 and alpha(v)beta5 integrin receptor antagonist. *Cancer Res.* 2001; **61**: 2232–2238.
33 Wiedlocha A, Sorensen V. Signaling, internalization, and intracellular activity of fibroblast growth factor. *Curr. Top. Microbiol. Immunol.* 2004; **286**: 45–79.
34 Rusnati M, Presta M. Interaction of angiogenic basic fibroblast growth factor with endothelial cell heparan sulfate proteoglycans. Biological implications in neovascularization. *Int. J. Clin. Lab. Res.* 1996; **26**: 15–23.
35 Presta M, Leali D, Stabile H, Ronca R, Camozzi M, Coco L. Heparin derivatives as angiogenesis inhibitors. *Curr. Pharm. Des.* 2003; **9**: 553–566.
36 Hassan HH. Chemistry and biology of heparin mimetics that bind to fibroblast growth factors. *Mini Rev. Med. Chem.* 2007; **7**(12): 1206–1235.

